scientific reports

Check for updates

OPEN

Direct shoulder MR arthrography using an iron-based positive T1 contrast agent (NEMO-103): comparison of image quality with gadolinium-based contrast

Hong Seon Lee[1,6], Chan Woong Jang[2,6], Young Han Lee[3], Sungjun Kim[1,4,5] & Jung Hyun Park[2,4,5]✉

The need for alternative MR contrast agents in direct shoulder MR arthrography (MRA) arises from limitations associated with gadolinium-based contrast agents (GBCAs), which are deemed "off-label" for MRA and raise concerns about potential toxicity to joint tissue. This study aims to compare the image quality of NEMO-103 (codename)-based and GBCA-based direct shoulder MRA. A total of 89 MRAs from 81 patients were analyzed, with 39 NEMO-103-based MRAs from 31 patients and 50 GBCA-based MRAs from 50 patients. The MRAs were performed at 3.0-T using fast/turbo spin-echo T1- and T2-weighted images with or without fat suppression (spectral presaturation with inversion recovery). Participants included individuals undergoing MRA for suspected or diagnosed shoulder pathologies between August 2021 and September 2022. Quantitative assessments (contrast-to-noise ratio [CNR] and distension measurements) and qualitative evaluations (distension, sharpness, contrast, and overall image quality scores) were conducted by three musculoskeletal radiologists. A visual Turing test (VTT) was used to assess the ability of 39 clinicians to differentiate between the two contrast agents. Statistical tests included the Shapiro–Wilk test, independent t-tests, and chi-squared test. The study compared 31 NEMO-103-based MRAs (11 females [35.5%], age: 40.0 ± 13.0 years) and 38 GBCA-based MRAs (14 females [36.8%], age: 49.4 ± 18.7 years) within 30 min post-injection, and 8 NEMO-103-based MRAs (3 females [37.5%], age: 38.0 ± 7.8 years) versus 12 GBCA-based MRAs (5 females [41.7%], age: 56.2 ± 15.7 years) in the 30–60-min post-injection timeframe. NEMO-103-based MRAs demonstrated superior axillary pouch distension and overall image quality in both comparisons. CNR was notably higher with NEMO-103. The VTT showed a 53.3% accuracy in differentiating NEMO-103 from GBCA, similar to random guessing. NEMO-103 may serve as a potential alternative to GBCAs for direct shoulder MRA, offering comparable or superior image quality with potentially fewer concerns related to gadolinium-associated toxicity.

Keywords Iron-based contrast agent, Gadolinium-based contrast agent, Direct shoulder MR arthrography, Visual Turing test

Gadolinium-based contrast agents (GBCAs) have been utilized in direct shoulder MR arthrography (MRA)[1–6], recognized for its high accuracy in evaluating intra-articular structures despite the invasiveness involved. Some practitioners opt for a saline-only approach to potentially reduce the risk of contrast reactions and achieve cost

[1]Department of Radiology, Gangnam Severance Hospital, Yonsei University College of Medicine, Seoul, Republic of Korea. [2]Department of Rehabilitation Medicine, Gangnam Severance Hospital, Rehabilitation Institute of Neuromuscular Disease, Yonsei University College of Medicine, 211, Eonju-ro, Gangnam-gu, Seoul, Republic of Korea. [3]Department of Radiology, Research Institute of Radiological Science and Center for Clinical Imaging Data Science, Severenace Hospital, Yonsei University College of Medicine, Seoul, Republic of Korea. [4]Department of Medical Device Engineering and Management, The Graduate School, Yonsei University College of Medicine, Seoul, Republic of Korea. [5]Department of Integrative Medicine, The Graduate School, Yonsei University College of Medicine, Seoul, Republic of Korea. [6]Hong Seon Lee and Chan Woong Jang contributed equally to this work. ✉email: RMPJH@yuhs.ac

savings[2,7–12]. However, advantages such as clearer delineation of intra-articular structures, improved signal-to-noise and contrast-to-noise ratios, attributed to the T1 shortening effects of diluted gadolinium, have been noted[13].

GBCAs have proven safety, stability, and efficacy over more than 30 years of use in various clinical settings[14–21]. However, in direct MRA, concerns have been raised by certain in vitro studies regarding potential adverse effects on chondrocytes[22], with conflicting findings reported[22–24]. Additionally, preclinical studies in rats have shown detectable levels of gadolinium in joint tissues following intra-articular injection of both linear and macrocyclic GBCAs[25], though the clinical significance of this is yet to be fully determined.

Efforts to find alternatives to GBCA have led to the development of non-GBCA, particularly iron-based or manganese-based ones, aiming to replace the T1 shortening effect[26,27]. Recently, an iron (Fe)-based contrast agent designed for direct MRA, NEMO-103 (codename), has been developed by Inventera Inc., Seoul, South Korea[28,29]. It comprises a biocompatible dextran core with an iron shell (supramolecular amorphous iron oxide) and has a molecular weight of approximately 32 kDa and like gadolinium, functions as a T1-positive contrast agent. Interestingly, NEMO-103 exhibits a longer joint cavity residence time (> 2 h) compared to typical GBCAs (~ 1 h) due to its larger molecular size. It is excreted from the joint cavity within 24 h after administration.

On the other hand, intra-articular injection of GBCAs lacks approval from the United States Food and Drug Administration and is considered an off-label use[13,30,31]. GBCAs need to be diluted hundreds of times for direct MRA, with the ideal concentration range for optimum signal-to-noise ratio being 1.25–2.5 mmol/L[32–35]. Injecting GBCAs outside the optimal concentration range (e.g., 0.7–3.4 mmol/L) inadvertently leads to a decrease in the signal of the injected substance[36]. However, NEMO-103 can be used directly without the need for dilution, eliminating concerns related to concentration variability.

While no studies have directly compared image quality between NEMO-103 and GBCAs, NEMO-103 is considered a promising alternative for direct shoulder MRA. The aim of this study is to demonstrate, through both objective and subjective evaluations that MRA using NEMO-103 are comparable to those obtained with GBCAs. Additionally, we aim to show superior image quality during the delayed phase (30–60 min post-injection), attributed to NEMO-103's longer joint-cavity residence times.

Materials and methods

Study design and data

The intra-articular administration of the investigational contrast agent NEMO-103 was conducted under a prospective clinical trial sponsored by Inventera Inc. (Trial ID: IVT_NEM_P1_20), which received prior approval from the Korean Ministry of Food and Drug Safety (MFDS). The present study is a retrospective secondary analysis of the imaging data obtained during that trial, and was separately approved by our institutional review board (No. 3-2023-0339). Informed consent was waived as the data were fully de-identified. All procedures were performed in accordance with the ethical standards of the Declaration of Helsinki.

A total of 138 direct shoulder MRAs from 90 patients were reviewed. After excluding 9 scans acquired at 120 min post-injection and 30 scans at 24 h post-injection (intended for pharmacokinetic analysis only), 99 MRAs remained eligible for image quality comparison. Two time-based comparison groups were defined: comparison 1 (0–30 min post-injection): 31 NEMO-103 MRAs versus 38 GBCA MRAs and Comparison 2 (30–60 min post-injection): 8 NEMO-103 MRAs versus 12 GBCA MRAs. Exclusion criteria included inadequate MR sequences, scanty intra-articular contrast agent (e.g., massive rotator cuff tear or technical error), or non-comparable scanner parameters (Fig. 1). All subjects in both the NEMO-103 and GBCA groups were symptomatic patients referred for clinical MRA due to suspected rotator cuff or labral pathology. No healthy volunteers were included.

Preparation of NEMO-103

NEMO-103 was synthesized according to a previously reported procedure[28,29]. Briefly, 20 mM Dextran T10 (551,000,109,001; Pharmacosmos) solution was mixed with a sodium hydroxide solution and epichlorohydrin (45,340; Sigma-Aldrich), followed by the addition of ethylenediamine (E26266; Sigma-Aldrich). The cross-linked dextran was purified via a 10 kDa cutoff ultrafiltration filter (UFC9010; Millipore). The terminal amine was further modified to form a carboxyl functional group. After ultrafiltration, the carboxyl-functionalized dextran was reacted with an iron chloride solution for 1 h. The final products were purified and concentrated by ultrafiltration.

Phantom study

Phantom images were acquired using a 3 T magnet machine (MAGNETOM Vida; Siemens Healthineers AG). Several concentrations of NEMO-103 and the GBCA (Dotarem®) were prepared (0.125, 0.25, 0.5, and 1.0 mM) in sealed tubes filled with 0.9% normal saline to minimize image artifacts. To obtain the MR relaxivities of NEMO-10 and GBCA, T1 (1) and T2 (2) mapping were performed as follows: (1) eight inversion times (TI) = [20, 100, 200, 400, 800, 1000, 2000, 4000] ms, repetition time (TR) = 4900 ms, echo time (TE) = 7 ms, average = 1, slice thickness = 1.0 mm, matrix size = 96 × 96, and field of view = 70 × 60 mm^2. (2) 15 TEs = [10, 20, 30, 40, 50, 60, 70, 80, 90, 100, 110, 120, 130, 140, 150] ms, TR = 3000 ms, average = 1, slice thickness = 1.0 mm, matrix size = 96 × 96, and field of view = 70 × 60 mm^2. T1 and T2 values were analyzed by drawing regions of interest (ROIs) in different tubes.

Direct shoulder MRA protocol

Under fluoroscopic guidance, test-injection with 3 mL of iodine contrast medium was done using a 20-gauge spinal needle to confirm the intra-articular position of the needle. Dotarem® was utilized as a representative GBCA and diluted 200-fold with saline before use, resulting in a final concentration of 2.5 mmol Gd/L. This dilution falls within the widely accepted optimal range of 1.25–2.5 mmol Gd/L for intra-articular use, as established in

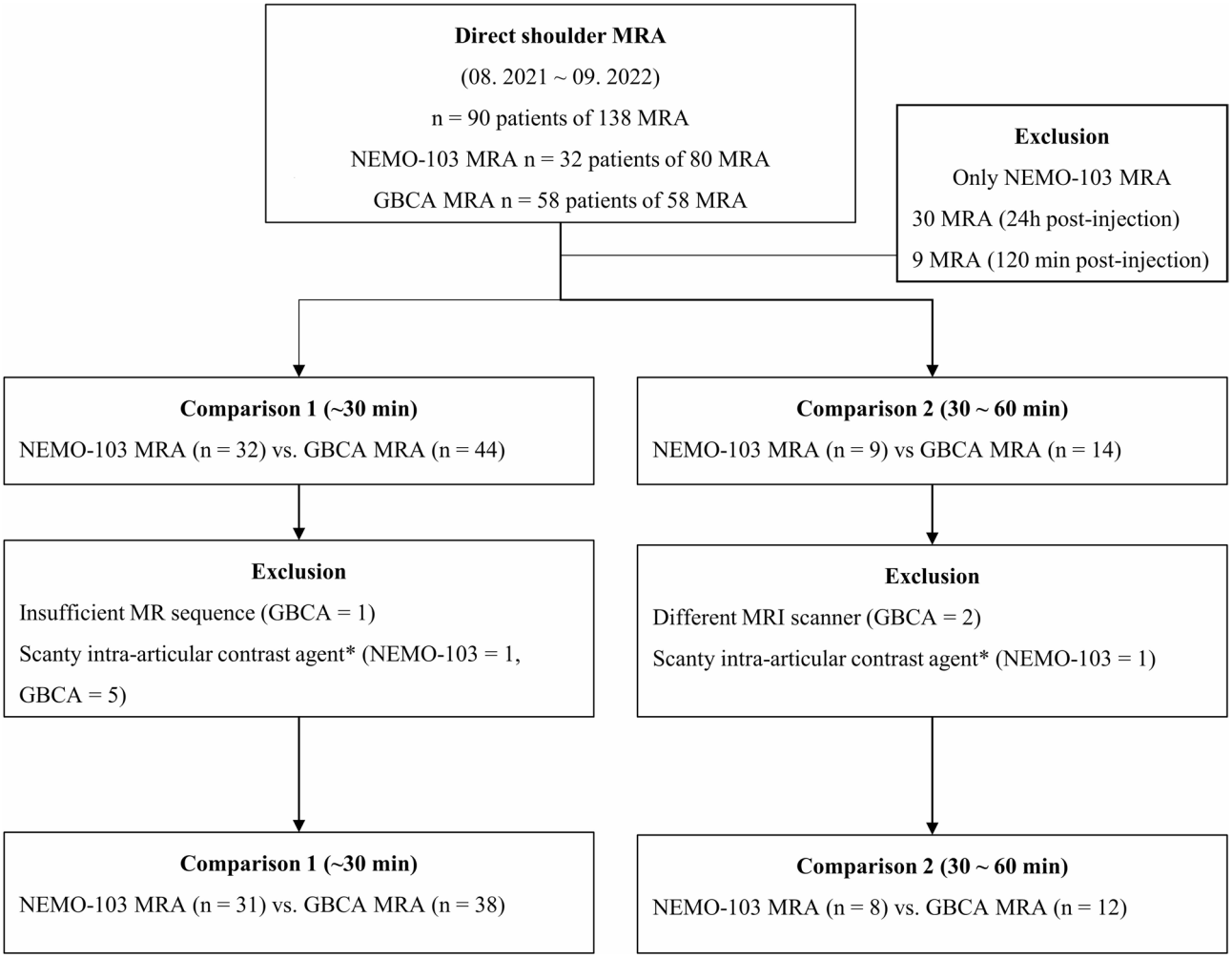

Fig. 1. Flow diagram of patient inclusion. *Due to technical error or massive rotator cuff tear. MRA, magnetic resonance arthrography.

Sequence	Orientation	TR/TE (ms)	NEx	Flip angle	Matrix size	FOV (mm^2)	ST/Gap (mm)	Fat suppression
T1-weighted SE	Axial	550/10	2	90°	256 × 256	140 × 140	2.5/0	SPIR
T1-weighted SE	Coronal	550/10	2	90°	256 × 256	140 × 140	2.5/0	SPIR
T1-weighted SE	Sagittal	550/10	2	90°	256 × 256	140 × 140	2.5/0	SPIR
T2-weighted SE	Coronal	3250/80	2	90°	256 × 256	140 × 140	2.5/0	SPIR

Table 1. MRI protocol. TR, repetition time; TE, echo time; SE, spin echo; FOV, field of view; SPIR, spectral presaturation with inversion recovery; ST, slice thickness; mm, millimeters; ms, milliseconds.

prior studies[32–35]. NEMO-103 was used without any additional manipulation, at a concentration of 2.5 mmol Fe/L. For all patients, approximately 12–15 mL of contrast agent was injected intra-articularly, which was halted if significant resistance occurred during the injection. All images were obtained using a 3.0 T Philips Achieva system (Philips Medical Systems). The imaging parameters were as follows: T1-weighted axial, sagittal, and coronal images with TR/TE = 550/10, flip angle = 90, matrix size = 256 × 256, field of view = 140 × 140 mm, number of excitations = 2, slice thickness = 2.5, no gap between slices, and fat suppression = spectral presaturation with inversion recovery. T2-weighted coronal images with TR/TE = 3250/80, flip angle = 90, matrix size = 256 × 256, field of view = 140 × 140 mm, number of excitations = 2, slice thickness = 2.5, no gap between slices, and fat suppression = spectral presaturation with inversion recovery. The same MR imaging protocol was applied to both contrast agent groups to ensure standardization and facilitate comparison. NEMO-103 was engineered to provide T1-shortening contrast similar to GBCAs, and phantom testing confirmed comparable relaxivity behavior. The parameters are summarized in Table 1.

Image quality assessment

We conducted both quantitative and qualitative image quality evaluations for all included images in Comparisons 1 and 2. All image sets were anonymized and stripped of clinical metadata, including patient age and diagnosis. The readers were blinded to the type of contrast agent and had access only to imaging data presented in randomized order. The quantitative measurements were done by board-certified musculoskeletal radiologists with 5 years of experience. For quantitative image quality assessment, we used the contrast-to-noise ratio (CNR) for each contrast agent[3]. The CNR of the intra-articular signal was calculated using the following equation:

$$CNR = \frac{(Signal\ Intensities\ in\ the\ ROIs - Signal\ Intensities\ in\ unenhanced\ muscle)}{SD\ of\ Background\ Noise}$$

The ROI was the axillary recess, adjacent to the articular surface of the humeral head. The signal intensity was evaluated by measuring the ROIs in the joint space and adjacent deltoid muscle tissue. The placement of the ROIs was repeated three times, and the CNR was averaged based on these measurements of signal intensity. The circular ROI was 100–200 mm^2 at the shoulder, and the standard deviation (SD) of the background noise was evaluated.

To assess the extent of distension, posterior and inferior capsular distension, and axillary pouch distension were measured. Posterior capsular distension was defined as the distance from the most posterior point of the glenoid bone to the most distended point of the posterior capsule at the mid-glenoid level in the MRA axial plane. Inferior capsular distension was defined as the distance from the most inferior point of the glenoid bone to the most distended point of the inferior capsule at the mid-glenoid level on MRA in the coronal plane. Axillary pouch distension involved measuring the most distended part of the axillary pouch in the mediolateral direction on the plane where inferior capsular distension was measured.

For qualitative image quality assessment[37] three board-certified musculoskeletal radiologists, each with 5, 16, and 20 years of clinical experience in direct shoulder MRA, independently and thoroughly reviewed multiple plane T1-weighted images. Each structure was evaluated in planes wherein it was clearly visible, and three criteria (distension, sharpness, and contrast) and overall image quality were used.

Distension was evaluated based on the delineation of the undersurface of the subscapularis muscles (SSC), long head biceps tendon (LHBT), and glenoid labrum; complete delineation, partial separation of the joint capsule and labrum, and inadequate delineation of the SSC, LHBT, and labrum received scores of 3, 2, and 1, respectively. Sharpness was evaluated based on the visual clarity and edge definition of key anatomical structures, including rotator cuff tendons, joint capsule, and labrum, on T1-weighted images.Scores of 3, 2, and 1 were assigned, respectively. The contrast was evaluated based on the delineation of the cartilage versus joint fluid. Scores of 3, 2, and 1 indicated good delineation, fair delineation, and inadequate delineation of cartilage versus joint fluid, respectively. The overall image quality was rated on a 5-point scale, with 5 indicating excellent image quality and 1 indicating poor image quality[3,38].

Visual Turing test[39–43]

Thirty-nine board-certified testers (35 musculoskeletal radiologists from various university hospitals, one orthopedic shoulder surgeon, and three specialists in musculoskeletal rehabilitation medicine), each with a ≥ 5 years of clinical experience, participated visual Turing test (VTT) for Comparison 1. Each radiologist received 30 sets of NEMO-103-based and GBCA-based shoulder MRA images within 30 min post-injection and had to determine independently, within a 30-s time limit, whether each image was based on NEMO-103. Each radiologist was blinded to the composition of the test sets, and the mean accuracy of the 39 experts was calculated for each task.

Statistical analysis

The normality of the variables was assessed using the Shapiro–Wilk test. Independent t-tests were used for continuous variables. The Chi-squared test was used to analyze categorical variables and compare differences between random guessing and the results of the VTT. Statistical significance was set at $p < 0.05$. All the statistical analyses were performed using SAS version 9.4 (SAS Institute).

Results

Baseline demographic data

Table 2 summarizes the basic demographic data of participants who underwent direct shoulder MRA, and Fig. 1 shows the participant selection. By Comparison 1, a comparative analysis was performed between a total of

	Comparison 1			Comparison 2		
	NEMO-103 (n = 31)	GBCA (n = 38)	*p*-value	NEMO-103 (n = 8)	GBCA (n = 12)	*p*-value
Age (year)*	40.0 ± 13.0	49.4 ± 18.7	0.020	38.0 ± 7.8	56.2 ± 15.7	0.008
Female (%)	11 (35.5)	14 (36.8)	0.907	3 (37.5)	5 (41.7)	1.000
Contrast volume (ml)*	14.0 ± 2.2	13.7 ± 1.8	0.539	11.3 ± 3.0	13.3 ± 1.6	0.112
Time (min)*/**	27.2 ± 5.7	24.5 ± 10.9	0.191	53.6 ± 2.7	52.6 ± 1.7	0.301

Table 2. Baseline demographic data. *Data are presented as mean ± standard deviation. **Time interval between the contrast injection and the time of MRI acquisition.

31 NEMO-based MRAs (11 females [35.5%]; age: 40.0 ± 13.0 years) and 38 GBCA-based MRAs (14 females [36.8%]; age: 49.4 ± 18.7 years) within 30 min post-injection. Comparison 2 entailed a comparison between the eight NEMO-based MRAs (3 females [37.5%]; age [mean ± SD]: 38.0 ± 7.8 years), and 12 GBCA-based MRAs (5 females [41.7%]; age: 56.2 ± 15.7 years) in 30–60 min post-injection. In Comparisons 1 and 2, wherein we assessed the quality of NEMO-103-based and GBCA-based shoulder MRA images in the same phases, the group that underwent NEMO-103-based shoulder MRA was notably younger ($p < 0.05$). No significant differences were observed regarding sex or amount of contrast agent used for the examination. Additionally, the time from contrast agent injection to MRA acquisition did not differ between the NEMO-103 and GBCA groups.

Phantom study

In the MRI performance test (Fig. 2), NEMO-103 exhibited a bright signal on T1-weighted MRI, similar to that of Dotarem® (Fig. 2a,b). The measured r_1 and r_2 values of NEMO-103 were 2.0 mM^{-1} s^{-1} and 2.3 mM^{-1} s^{-1}, respectively (Fig. 2c, e). The r_2/r_1 ratio of NEMO-103 was 1.15, which is within the favorable range for T1 MRI contrast agents. A low r2/r1 ratio, typically between 1 and 2, indicates a predominant T1 effect and minimal T2 interference, which is desirable for enhancing signal intensity on T1-weighted images[44,45]. By comparison, the r_1, r_2, and r_2/r_1 ratio of Dotarem® were 4.7 mM^{-1} s^{-1}, 5.2 mM^{-1} s^{-1}, and 1.11, respectively. These results indicate that despite being an iron-based contrast agent, NEMO-103 exhibits a decent T1 contrast effect; additionally, its performance was comparable to that of traditional GBCAs.

Image quality assessment

Table 3 and Fig. 3 show the results of the image quality assessment. When comparing NEMO-103-based and GBCA-based shoulder MRA images in Comparison 1, no differences were observed in CNR; however, a significant

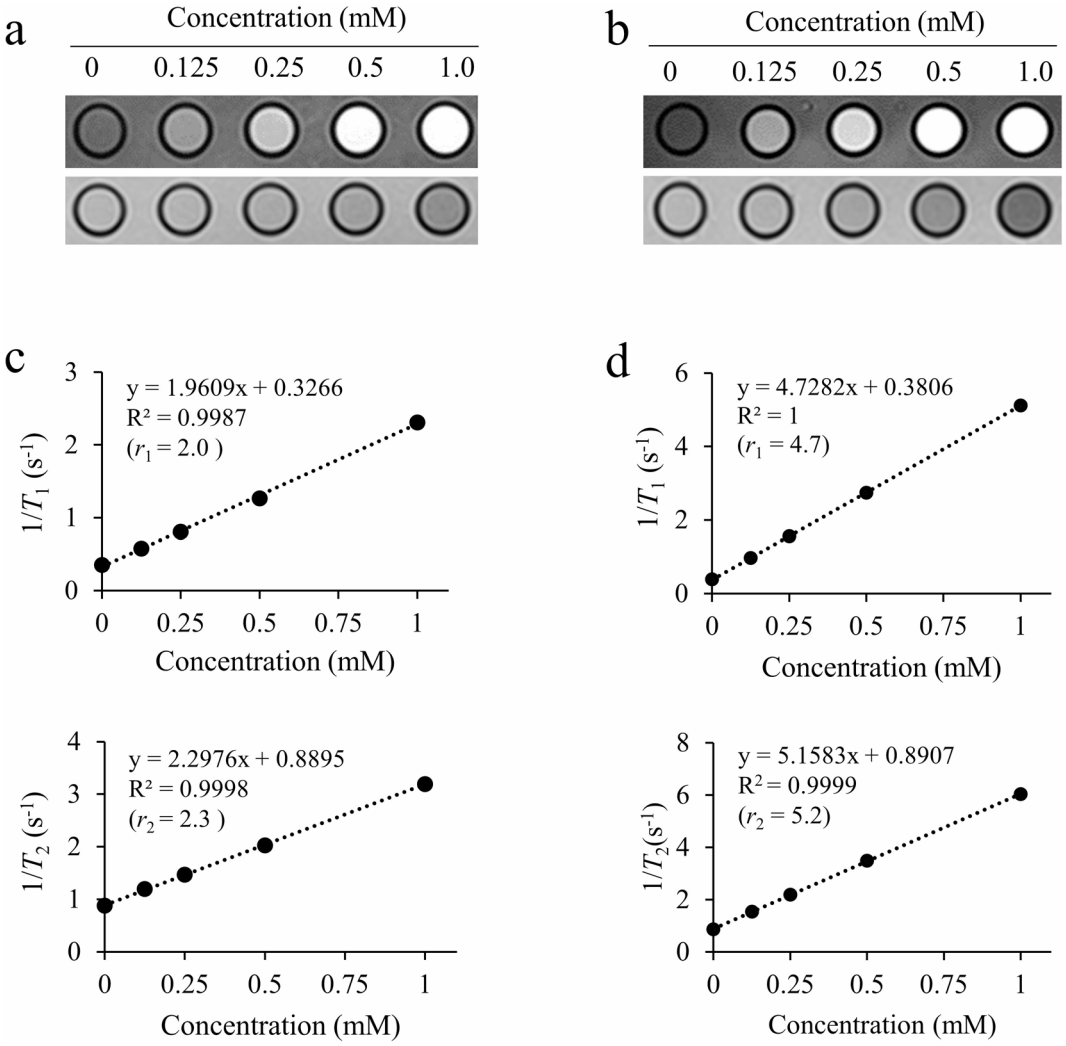

Fig. 2. Schematic of structure and MR imaging performance of NEMO-103. (**a**) Structure of NEMO-103. (**b**, **c**) T1 (top)- and T2 (bottom)-weighted images for NEMO-103 (**b**) and GBCA (Dotarem) (**c**) containing phantoms obtained using a 3.0 T MRI scanner. (**d**,**e**) T1 (top) and T2 (bottom) relaxivity plots for NEMO-103 (**d**) and GBCA (**e**). GBCA, gadolinium-based contrast agent

	Comparison 1 (0 ~ 30 min)			Comparison 2 (30 ~ 60 min)		
	NEMO-103 (n = 31)	GBCA (n = 38)	*p*-value	NEMO-103 (n = 8)	GBCA (n = 12)	*p*-value
Contrast to noise ratio	112.3 ± 44.6	127.3 ± 41.4	0.154	92.9 ± 26.7	61.5 ± 29.7	0.027
Posterior capsular distension (mm)	13.9 ± 3.6	13.1 ± 2.7	0.311	13.0 ± 4.2	12.4 ± 3.1	0.716
Inferior capsular distension (mm)	10.9 ± 2.6	8.0 ± 5.2	0.004	11.0 ± 2.9	5.8 ± 6.2	0.044
Axillary pouch distension (mm)	9.9 ± 4.6	6.7 ± 4.8	0.006	9.9 ± 3.7	4.5 ± 5.6	0.029
Subjective assessment (range)						
Overall image quality (1–5)	4.7 ± 0.5	4.4 ± 0.5	0.034	4.9 ± 0.2	4.2 ± 0.9	0.020
Distension (1–3)	2.8 ± 0.3	2.6 ± 0.4	0.024	3.0 ± 0.0	2.3 ± 0.9	0.025
Sharpness (1–3)	2.7 ± 0.4	2.5 ± 0.3	0.059	2.8 ± 0.3	2.5 ± 0.5	0.090
Contrast (1–3)	3.0 ± 0.0	2.9 ± 0.2	0.051	3.0 ± 0.0	2.7 ± 0.5	0.039

Table 3. Quantitative and qualitative image quality assessment in Comparisons 1 and 2. *Data are presented as mean ± standard deviation.

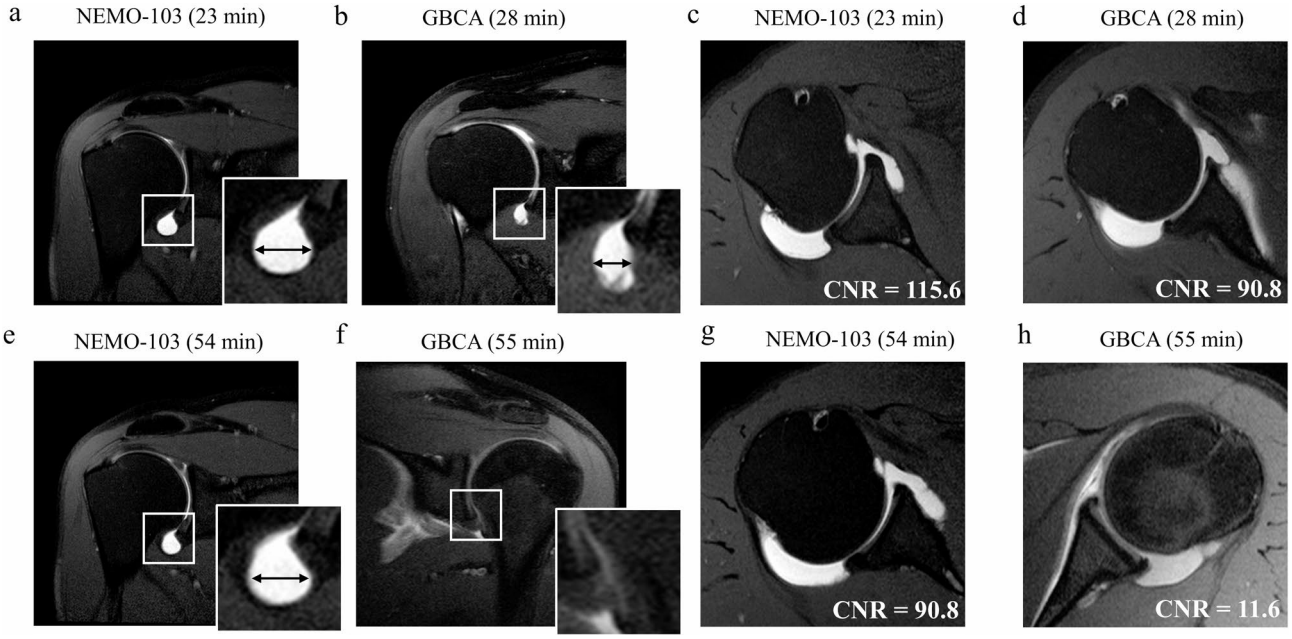

Fig. 3. Differences in the distension and CNR between the NEMO-103 and the GBCA. The first column (**a**–**d**) represents Comparison 1, which compares MRAs conducted within 30 min post-injection. The second column (**e**–**h**) represents Comparison 2, which compares MRAs conducted between 30 and 60 min post-injection. (**a**, **c**) Coronal and axial T1-weighted images from NEMO-103-based shoulder MRA of a 47-year-old male in 23 min post-injection, and (**b**, **d**) GBCA-based shoulder MRA images of a 42-year-old male in 28 min post-injection. The CNR values (115.6 vs. 90.8) of the two images were comparable (**c**, **d**); however, a noticeable reduction in the axillary pouch distension (black arrows in **a**, **b**) was observed in the GBCA (10.5 mm vs. 5.5 mm). (**e**, **g**) Coronal and axial T1-weighted images from NEMO-103-based shoulder MRA of a 47-year-old male in 54 min post-injection, and (**f**, **h**) GBCA-based shoulder MRA images of a 19-year-old male in 55 min post-injection. Direct shoulder MRA using the NEMO-103 maintained axillary pouch distension (9.9 mm, **e**), whereas the axillary pouch was completely obliterated in the GBCA-based direct shoulder MRA (**f**). The CNR was significantly higher for NEMO-103 (90.8 vs. 11.6) (**g**, **h**). CNR, contrast-to-noise ratio; GBCA, gadolinium-based contrast agent; MRA, magnetic resonance arthrography.

difference in inferior capsular (10.9 ± 2.6 mm vs. 8.0 ± 5.2 mm, $p = 0.004$) and axillary pouch (9.9 mm ± 4.6 vs 6.7 mm ± 4.8, $p = 0.006$) distension was found. Thus, NEMO-103-based shoulder MRA images achieved higher mean scores for overall image quality (4.7 ± 0.5 vs. 4.4 ± 0.5; $p = 0.034$). There was no significant difference in the posterior capsular distension between the two groups (13.9 ± 3.6 mm vs. 13.1 ± 2.7 mm; $p = 0.311$).

In Comparison 2, more prominent differences were observed. The CNR was significantly higher in NEMO-103-based than GBCA-based shoulder MRA (92.9 ± 26.7 vs. 61.5 ± 29.7; $p = 0.027$). Additionally, more pronounced differences in inferior capsular (11.0 ± 2.9 mm vs. 5.8 ± 6.2 mm, $p = 0.044$) and axillary pouch (9.9 ± 3.7 mm vs. 4.5 ± 5.6 mm; $p = 0.029$) distension were observed. As a result, NEMO-103-based shoulder MRA images achieved higher mean scores in overall image quality (4.9 ± 0.2 vs. 4.2 ± 0.9; $p = 0.020$). There was

no significant difference in posterior capsular distension between the two groups (13 ± 4.2 mm vs. 12.4 ± 3.1 mm; $p = 0.716$).

VTT

In the VTT for Comparison 1, radiologists were tasked with distinguishing between NEMO-103-based and GBCA-based shoulder MRA images within 30 min post-injection. The combined accuracy of the 39 testers averaged 53.3% (624/1170), and there was no statistically significant difference compared with random guessing (50.0%, 585/1170; $p = 0.107$).

Discussion

Safety concerns regarding GBCAs have prompted exploration into iron-based alternatives; thus, we assessed the efficacy of NEMO-103 in direct shoulder MRA. MRA following the direct intra-articular injection of iron or gadolinium revealed nearly identical image quality regarding CNR and VTT results. Additionally, NEMO-103 demonstrated an enhanced CNR at 30–60 min post-injection, suggesting the extension of the feasible post-injection imaging time window. In patients with bilateral conditions (like rotator cuff disease)[46] undergoing consecutive GBCA-based MRA, the side imaged later may exhibit a suboptimal CNR or distension. Thus, this finding may increase the operational efficiency of MR facilities in clinical practice.

Our findings suggest that NEMO-103, particulate contrast agents with a hydrodynamic diameter of 3 nm, are excreted from the joint cavity by lymphatic vessels, and are not cleared by the veins due to their larger size[47,48]; thus, NEMO-103 can only be excreted by the lymphatic vessels, leading to extended retention in the joint cavity. Contrastingly, GBCAs (< 1 nm) are rapidly cleared through both the lymphatic vessels and veins. Still, complete clearance of NEMO-103 from the joint cavity was confirmed, with no residual presence detected in the MRA images acquired 24 h post-administration.

There was no significant difference in posterior capsular distension between the NEMO-103 and GBCA groups, likely owing to the patient's position during MRA. In the supine position, the joint fluid tends to shift towards the posterior capsule, resulting in relatively less residual fluid in structures like the subscapularis tendons' undersurface, and axillary pouch. Eventually, as the contrast agent is resorbed, this difference becomes more pronounced when using GBCA. Consequently, GBCA exhibited a relatively higher incidence of axillary pouch obliteration than NEMO-103. Moreover, the anterior aspect of the glenohumeral joint contains critical structures[49]; given the multitude of structures that need to be assessed in this region, the resorption of joint fluid and positional shift of fluid due to position may affect the conspicuity of lesions in this region.

Unlike the well-established use of GBCAs over time[21] NEMO-103 requires safety assessment. In our study, no serious adverse events were observed. However, this sample size is insufficient to make definitive claims regarding its safety. Three out of 32 subjects (9.4%) who underwent NEMO-103-based shoulder MRA reported treatment-emergent events including muscle pain (n = 2) and transient hypertension (n = 1). These events were self-limiting and resolved without intervention. Investigators classified these as unlikely to be related to the investigational drug based on clinical judgment, considering pre-existing conditions, lack of dose–response relationship, and plausible alternative explanations. Safety monitoring in the original clinical trial included clinical laboratory tests (complete blood count, liver and renal function, electrolytes, and iron panel), vital signs (blood pressure, heart rate, and body temperature), electrocardiography, and physical examination. In addition, liver and spleen MRI was performed 24 h post-injection to evaluate systemic retention of iron. No clinically significant abnormalities were observed in any of these parameters. As such, further studies with comprehensive safety monitoring are warranted to assess the causal relationship more rigorously. Although our study observed no serious adverse events associated with NEMO-103, its long-term toxicity profile in humans remains unknown. Given the absence of post-marketing surveillance data and long-term follow-up studies, caution is warranted regarding potential risks such as iron accumulation or deposition following repeated or high-dose use. Further longitudinal studies are needed to evaluate the chronic safety of NEMO-103.

Another advantage of NEMO-103 is its potential to divert from traditional off-label use. Conventional GBCA-based shoulder MRA involves the cumbersome process of diluting GBCA to approximately 1:200[50] increasing the risk of hindering standardization of the contrast agent concentration. Conversely, NEMO-103 is supplied at the appropriate concentration for MR arthrography, offering relative freedom from issues including infection, contamination, and contrast agent concentration heterogeneity. Despite the promising image quality, iron-based contrast agents such as NEMO-103 are not yet widely adopted. Contributing factors may include limited regulatory approval, unfamiliarity among radiologists, insufficient long-term safety data, and concerns about potential iron overload, particularly in repeated or systemic use. Additionally, standardization of imaging protocols for iron-based agents remains underexplored.

Owing to the retrospective design and limited number of patients, this study had several limitations. First, patients who underwent arthrography were not surgically targeted; therefore, the diagnostic accuracy for each lesion in both shoulder MRAs could not be assessed with reference of arthroscopic finding. However, by emphasizing the role of the contrast agent within the joint cavity, including the enhancement of contrast between surrounding structures and joint cavity distension, significant differences between NEMO-103 and GBCA were observed over time. Additionally, through a VTT involving many testers, NEMO-103 demonstrated an image quality equal to that of GBCA from various perspectives. Future clinical trials should involve patients requiring surgery and utilize their surgical records as the gold standard to evaluate the diagnostic accuracy of the two contrast agents. Second, we did not evaluate contrast agents administered to the same patient. Individual differences may exist in joint cavity distension and contrast agent resorption; however, performing two MRAs with different contrast agents on the same patient within a short timeframe is challenging. To overcome this limitation, the time from contrast agent injection to MRA acquisition was carefully examined using phase matching. Third, the GBCA group was significantly older than the NEMO-103 group. Although unproven,

there may be a difference in the rate of contrast agent resorption with age; however, considering that synovial fluid tends to increase with more severe degeneration and symptoms like pain[51,52] it is plausible that the GBCA patient group may have had a larger synovial fluid volume than the relatively younger, volunteer-based NEMO-103 group. Forth, it should also be noted that CNR measurements in a multi-channel coil setup are inherently limited due to the presence of vendor-specific image reconstruction and noise-normalization algorithms, which may introduce variability or overestimate signal homogeneity. Therefore, CNR values should be interpreted with caution and primarily as relative, not absolute, indicators of contrast performance. Fifth, although relaxivity was measured in normal saline rather than biological fluid in the phantom study, future studies are warranted to assess relaxivity in serum or synovial environments to better reflect in vivo behavior. Last, despite its low dosage, potential issues—including iron overload or deposition with extensive and repetitive use—are possible owing to the lack of post-marketing surveillance data for NEMO-103; however, this was not investigated.

In conclusion, NEMO-103 is comparable with GBCA regarding CNR, distension, subjective image quality, and VTT results. Additionally, it exhibited enhanced resistance to contrast resorption over time, thereby potentially extending the imaging time window.

Data availability

The datasets used and/or analysed during the current study available from the corresponding author on reasonable request.

Received: 8 October 2024; Accepted: 20 May 2025
Published online: 02 July 2025

References

1. El-Liethy, N., Kamal, H. & Elsayed, R. F. Role of conventional MRI and MR arthrography in evaluating shoulder joint capsulolabral-ligamentous injuries in athletic versus non-athletic population. *Egypt. J. Radiol. Nuclear Med.* **47**, 969–984 (2016).
2. Helms, C. A., McGonegle, S. J., Vinson, E. N. & Whiteside, M. B. Magnetic resonance arthrography of the shoulder: Accuracy of gadolinium versus saline for rotator cuff and labral pathology. *Skeletal Radiol.* **40**, 197–203 (2011).
3. Duc, S. R., Froehlich, J. M., Gustav Hodler, J. & Weishaupt, D. MR arthrography of the shoulder, hip, and wrist: Evaluation of contrast dynamics and image quality with increasing injection-to-imaging time. *Am. J. Roentgenol.* **188**, 1081–1088 (2007).
4. Zanetti, M., Jost, B., Lustenberger, A. & Hodler, J. Clinical impact of MR arthrography of the shoulder. *Acta Radiol.* **40**, 296–302 (1999).
5. Hahn, O. H. C., Schweitzer, M. E. & Spettell, C. M. Internal derangements of the shoulder: decision tree and cost-effectiveness analysis of conventional arthrography, conventional MRI, and MR arthrography. *Skelet. Radiol.* **28**, 670–678 (1999).
6. Flannigan, B. et al. MR arthrography of the shoulder: Comparison with conventional MR imaging. *AJR Am. J. Roentgenol.* **155**, 829–832 (1990).
7. Singer, A. D. et al. A comparison of saline and gadolinium shoulder MR arthrography to arthroscopy. *Skeletal Radiol.* **49**, 625–633 (2020).
8. Tornetta, P. III. et al. How effective is a saline arthrogram for wounds around the knee?. *Clin. Orthop. Relat. Res.* **466**, 432–435 (2008).
9. Willemsen, U. et al. Prospective evaluation of MR arthrography performed with high-volume intraarticular saline enhancement in patients with recurrent anterior dislocations of the shoulder. *AJR Am. J. Roentgenol.* **170**, 79–84 (1998).
10. Zanetti, M. & Hodler, J. Contrast media in MR arthrography of the glenohumeral joint: intra-articular gadopentetate vs saline: Preliminary results. *Eur. Radiol.* **7**, 498–502 (1997).
11. Schwartz, M. L., Al-Zahrani, S., Morwessel, R. M. & Andrews, J. R. Ulnar collateral ligament injury in the throwing athlete: Evaluation with saline-enhanced MR arthrography. *Radiology* **197**, 297–299 (1995).
12. Tirman, P. F. et al. Saline magnetic resonance arthrography in the evaluation of glenohumeral instability. *Arthrosc. J. Arthrosc. Relat. Surg.* **9**, 550–559 (1993).
13. Chang, E. Y. et al. SSR white paper: Guidelines for utilization and performance of direct MR arthrography. *Skeletal Radiol.* **53**, 209–244 (2024).
14. Kanal, E. Gadolinium based contrast agents (GBCA): Safety overview after 3 decades of clinical experience. *Magn. Reson. Imaging* **34**, 1341–1345 (2016).
15. Lancelot, E., Raynaud, J.-S. & Desché, P. Current and future MR contrast agents: Seeking a better chemical stability and relaxivity for optimal safety and efficacy. *Invest. Radiol.* **55**, 578–588 (2020).
16. Do, C. et al. Gadolinium-based contrast agent use, their safety, and practice evolution. *Kidney360* **1**, 561–568 (2020).
17. Lum, M. & Tsiouris, A. J. MRI safety considerations during pregnancy. *Clin. Imaging* **62**, 69–75 (2020).
18. Patel, M., Atyani, A., Salameh, J.-P., McInnes, M. & Chakraborty, S. Safety of intrathecal administration of gadolinium-based contrast agents: A systematic review and meta-analysis. *Radiology* **297**, 75–83 (2020).
19. Cowling, T. & Frey, N. Macrocyclic and linear gadolinium based contrast agents for adults undergoing magnetic resonance imaging: A review of safety. (2019).
20. Goischke, H.-K. Safety assessment of gadolinium-based contrast agents (GBCAs) requires consideration of long-term adverse effects in all human tissues. *Mult. Scler. J. Exp. Trans. Clin.* **3**, 2055217317704450 (2017).
21. Runge, V. M. Safety of the gadolinium-based contrast agents for magnetic resonance imaging, focusing in part on their accumulation in the brain and especially the dentate nucleus. *Invest. Radiol.* **51**, 273–279 (2016).
22. Greisberg, J. K., Wolf, J. M., Wyman, J., Zou, L. & Terek, R. M. Gadolinium inhibits thymidine incorporation and induces apoptosis in chondrocytes. *J. Orthop. Res.* **19**, 797–801 (2001).
23. Midura, S. et al. In vitro toxicity in long-term cell culture of MR contrast agents targeted to cartilage evaluation. *Osteoarthrit. Cartil.* **22**, 1337–1345 (2014).
24. Oznam, K. et al. Iopromide-and gadopentetic acid-derived preparates used in MR arthrography may be harmful to chondrocytes. *J. Orthop. Surg. Res.* **12**, 1–10 (2017).
25. Brown, R. R., Clarke, D. W. & Daffner, R. H. Is a mixture of gadolinium and iodinated contrast material safe during MR arthrography?. *Am. J. Roentgenol.* **175**, 1087–1090 (2000).
26. Davis, K. A. & Lazar, B. Manganese-based contrast agents as a replacement for gadolinium. *Radiol. Technol.* **93**, 36–45 (2021).
27. Boehm-Sturm, P. et al. Low-molecular-weight iron chelates may be an alternative to gadolinium-based contrast agents for T1-weighted contrast-enhanced MR imaging. *Radiol.* **286**, 537–546 (2018).
28. Shin, T.-H. et al. High-resolution T1 MRI via renally clearable dextran nanoparticles with an iron oxide shell. *Nat. Biomed. Eng.* **5**, 252–263 (2021).

29. Kim, J.-W. et al. Iron oxide-coated dextran nanoparticles with efficient renal clearance for musculoskeletal magnetic resonance imaging. *ACS Appl. Nano Mater.* **4**, 12943–12948 (2021).
30. Runge, V. M. & Knopp, M. V. Off-label use and reimbursement of contrast media in MR. *J. Magn. Reson. Imag. Off. J. Int. Soc. Magn. Resonan. Med.* **10**, 489–495 (1999).
31. Kralik, S. F., Singhal, K. K., Frank, M. S. & Ladd, L. M. Evaluation of gadolinium deposition in the brain after MR arthrography. *Am. J. Roentgenol.* **1211**, 063–1067 (2018).
32. Sebro, R., Oliveira, A. & Palmer, W. E. MR arthrography of the shoulder: technical update and clinical applications. in *Seminars in musculoskeletal radiology*, Vol. 18 352–364 (Thieme Medical Publishers, 2014).
33. Jbara, M., Chen, Q., Marten, P., Morcos, M. & Beltran, J. Shoulder MR arthrography: how, why, when. *Radiol. Clin.* **43**, 683–692 (2005).
34. Chung, C. B., Corrente, L. & Resnick, D. MR arthrography of the shoulder. *Magn. Reson. Imaging Clin.* **12**, 25–38 (2004).
35. Petersilge, C. A., Lewin, J. S., Duerk, J. L. & Hatem, S. F. MR arthrography of the shoulder: Rethinking traditional imaging procedures to meet the technical requirements of MR imaging guidance. *AJR Am. J. Roentgenol.* **169**, 1453–1457 (1997).
36. Andreisek, G. et al. Direct MR arthrography at 1.5 and 3.0 T: Signal dependence on gadolinium and iodine concentrations—Phantom study. *Radiology* **247**, 706–716 (2008).
37. Andreisek, G., Duc, S. R., Froehlich, J. M., Hodler, J. & Weishaupt, D. MR arthrography of the shoulder, hip, and wrist: Evaluation of contrast dynamics and image quality with increasing injection-to-imaging time. *Am. J. Roentgenol.* **188**, 1081–1088 (2007).
38. Berquist, T. H. Imaging of articular pathology: MRI, CT, arthrography. *Clin. Anat. Off. J. Am. Assoc. Clin. Anat. Br. Assoc. Clin. Anat.* **10**, 1–13 (1997).
39. Myong, Y. et al. Evaluating diagnostic content of AI-generated chest radiography: A multi-center visual Turing test. *PLoS ONE* **18**, e0279349 (2023).
40. Yenneti, S. S. S. *Visual Turing Test for Generative Models in Medical Imaging* (State University of New York, 2022).
41. Hong, K.-T. et al. Lumbar spine computed tomography to magnetic resonance imaging synthesis using generative adversarial network: Visual turing test. *Diagnostics* **12**, 530 (2022).
42. Park, H. Y. et al. Realistic high-resolution body computed tomography image synthesis by using progressive growing generative adversarial network: Visual turing test. *JMIR Med. Inform.* **9**, e23328 (2021).
43. Chuquicusma, M. J., Hussein, S., Burt, J. & Bagci, U. How to fool radiologists with generative adversarial networks? A visual turing test for lung cancer diagnosis. In *2018 IEEE 15th International Symposium on Biomedical Imaging (ISBI 2018)* 240–244 (IEEE, 2018).
44. Caravan, P., Ellison, J. J., McMurry, T. J. & Lauffer, R. B. Gadolinium(III) chelates as MRI contrast agents: Structure, dynamics, and applications. *Chem. Rev.* **99**, 2293–2352 (1999).
45. Estelrich, J., Escribano, E., Queralt, J. & Busquets, M. A. Iron oxide nanoparticles for magnetically-guided and magnetically-responsive drug delivery. *Int. J. Mol. Sci.* **16**, 8070–8101 (2015).
46. Yamaguchi, K. et al. The demographic and morphological features of rotator cuff disease. A comparison of asymptomatic and symptomatic shoulders. *J. Bone Joint. Surg. Am.* **88**, 1699–1704 (2006).
47. Müller, A. et al. Magnetic resonance lymphography at 9.4 t using a gadolinium-based nanoparticle in rats: Investigations in healthy animals and in a hindlimb lymphedema model. *Invest. Radiol.* **52**, 725–733 (2017).
48. Kobayashi, H. et al. Delivery of gadolinium-labeled nanoparticles to the sentinel lymph node: Comparison of the sentinel node visualization and estimations of intra-nodal gadolinium concentration by the magnetic resonance imaging. *J. Control Release* **111**, 343–351 (2006).
49. Llopis, E., Pau Montesinos, M., Guedez, L. A. & Cerezal, L. Normal shoulder MRI and MR arthrography: Anatomy and technique. *Semin. Musculoskelet. Radiol.* **19**(03), 212–230. https://doi.org/10.1055/s-0035-1549316 (2015).
50. Blomqvist, L., Nordberg, G. F., Nurchi, V. M. & Aaseth, J. O. Gadolinium in medical imaging-usefulness, toxic reactions and possible countermeasures-a review. *Biomolecules* **12**, 742 (2022).
51. Gait, A. D. et al. Synovial volume vs synovial measurements from dynamic contrast enhanced MRI as measures of response in osteoarthritis. *Osteoarthr. Cartil.* **24**, 1392–1398 (2016).
52. Kraus, V. B., Stabler, T. V., Kong, S. Y., Varju, G. & McDaniel, G. Measurement of synovial fluid volume using urea. *Osteoarthr. Cartil.* **15**, 1217–1220 (2007).

Acknowledgements

This research was supported by Korea Drug Development Fund funded by Ministry of Science and ICT, Ministry of Trade, Industry, and Energy, and Ministry of Health and Welfare (RS-2023-00282888, Republic of Korea).

Author contributions

Conceptualization was performed by JHP; methodology was done by HSL, CWJ; formal analysis was provided by HSL, CWJ; data curation was gathered by HSL, SK, YHL; writing was done by HSL, CWJ; review & editing did by SK, YHL, JHP; supervision was conducted by SK, YHL, JHP.

Declarations

Competing interests

The authors declare no competing interests.

Additional information

Correspondence and requests for materials should be addressed to J.H.P.